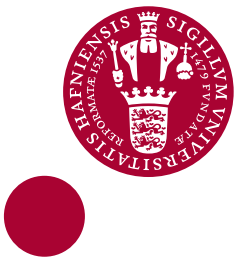

Snowpack fluxes of methane and carbon dioxide from high Arctic tundra

Pirk, Norbert; Tamstorf, Mikkel P.; Lund, Magnus; Mastepanov, Mikhail; Pedersen, Stine Helene Falsig; Mylius, Maria Rask; Parmentier, Frans-Jan W.; Christiansen, Hanne Hvidtfeldt; Christensen, Torben R.

Published in:
Journal of Geophysical Research: Biogeosciences

DOI:
10.1002/2016JG003486

Publication date:
2016

Document version
Publisher's PDF, also known as Version of record

AGU PUBLICATIONS

JGR

Journal of Geophysical Research: Biogeosciences

RESEARCH ARTICLE
10.1002/2016JG003486

Key Points:
- Small gas fluxes from the frozen soil resemble the same spatial pattern as during the growing season
- Snowpack ice layers block the diffusive fluxes leading to high snowpack gas concentrations
- In polygonal tundra, geomorphological soil cracks are the strongest methane source during wintertime

Supporting Information:
- Supporting Information S1

Correspondence to:
N. Pirk,
norbert.pirk@nateko.lu.se

Citation:
Pirk, N., M. P. Tamstorf, M. Lund, M. Mastepanov, S. H. Pedersen, M. R. Mylius, F.-J. W. Parmentier, H. H. Christiansen, and T. R. Christensen (2016), Snowpack fluxes of methane and carbon dioxide from high Arctic tundra, *J. Geophys. Res. Biogeosci.*, *121*, 2886–2900, doi:10.1002/2016JG003486.

Received 13 MAY 2016
Accepted 6 NOV 2016
Accepted article online 14 NOV 2016
Published online 25 NOV 2016

Snowpack fluxes of methane and carbon dioxide from high Arctic tundra

Norbert Pirk[1,2], Mikkel P. Tamstorf[3], Magnus Lund[3], Mikhail Mastepanov[1,3], Stine H. Pedersen[3], Maria R. Mylius[4], Frans-Jan W. Parmentier[1,3], Hanne H. Christiansen[2], and Torben R. Christensen[1,3]

[1]Department of Physical Geography and Ecosystem Science, Lund University, Lund, Sweden, [2]Geology Department, University Centre in Svalbard, UNIS, Longyearbyen, Norway, [3]Arctic Research Centre, Bioscience, Aarhus University, Roskilde, Denmark, [4]Department of Geosciences and Natural Resource Management, University of Copenhagen, Copenhagen, Denmark

Abstract Measurements of the land-atmosphere exchange of the greenhouse gases methane (CH_4) and carbon dioxide (CO_2) in high Arctic tundra ecosystems are particularly difficult in the cold season, resulting in large uncertainty on flux magnitudes and their controlling factors during this long, frozen period. We conducted snowpack measurements of these gases at permafrost-underlain wetland sites in Zackenberg Valley (NE Greenland, 74°N) and Adventdalen Valley (Svalbard, 78°N), both of which also feature automatic closed chamber flux measurements during the snow-free period. At Zackenberg, cold season emissions were 1 to 2 orders of magnitude lower than growing season fluxes. Perennially, CH_4 fluxes resembled the same spatial pattern, which was largely attributed to differences in soil wetness controlling substrate accumulation and microbial activity. We found no significant gas sinks or sources inside the snowpack but detected a pulse in the δ^{13}C-CH_4 stable isotopic signature of the soil's CH_4 source during snowmelt, which suggests the release of a CH_4 reservoir that was strongly affected by methanotrophic microorganisms. In the polygonal tundra of Adventdalen, the snowpack featured several ice layers, which suppressed the expected gas emissions to the atmosphere, and conversely lead to snowpack gas accumulations of up to 86 ppm CH_4 and 3800 ppm CO_2 by late winter. CH_4 to CO_2 ratios indicated distinctly different source characteristics in the rampart of ice-wedge polygons compared to elsewhere on the measured transect, possibly due to geomorphological soil cracks. Collectively, these findings suggest important ties between growing season and cold season greenhouse gas emissions from high Arctic tundra.

1. Introduction

Fluxes of methane (CH_4) and carbon dioxide (CO_2) from Arctic tundra exhibit tremendous spatial variability due to complex microtopography [*Sturtevant and Oechel*, 2013; *Olefeldt et al.*, 2013]. The large associated variations in soil wetness, temperature, and vegetation composition lead to varying rates of respiratory releases and microbial decomposition of organic material. Most measurements of the above are performed during the growing season, while much fewer studies exist that explain the magnitude and controls of wintertime emissions [*McGuire et al.*, 2012].

Most biological activity in permafrost-underlain soils takes place in the uppermost, seasonally unfrozen part of the soil (also known as the active layer), whose thickness and wetness is a key control on gas exchange processes [*Christensen et al.*, 2003; *Whalen*, 2005]. Under waterlogged, anaerobic, conditions CH_4 is produced by methanogenic microorganisms, while methanotrophic microorganisms in the aerobic part of the soil consume CH_4 as part of their metabolism [*Lai*, 2009]. The underlying microbial processes fractionate the carbon isotopes in distinctive ways, which can be studied by measuring the stable isotopic composition of CH_4 [*Hornibrook et al.*, 2000; *Preuss et al.*, 2013; *Vaughn et al.*, 2016]. Water table position also has an indirect effect on the gas exchange since it controls the abundance of vascular plants, which have been found to affect carbon turnover and CH_4 emissions through their root exudates and plant mediated gas transport [*Schimel*, 1995; *Ström et al.*, 2005].

The majority of studies on Arctic greenhouse gas dynamics have focused on the growing season, even though this season covers a mere 2 to 3 months of the year [*McGuire et al.*, 2012]. The present study, on the other hand, focuses on the much longer Arctic winter, which can be classified into several periods based on the

prevailing climatological and thermophysical conditions [*Olsson et al.*, 2003]. Accordingly, we refer to the time from the end of the autumnal active layer freeze-in to the beginning of ground thawing after snowmelt as the cold season (typically November–May for high Arctic sites). The autumnal freeze-in can feature sudden emission bursts, which have been suggested to be related to the physical release of stored gases through frost-induced ground fissures [*Mastepanov et al.*, 2008, 2013; *Pirk et al.*, 2015]. Once the active layer is completely frozen, the photosynthetic carbon assimilation typically ceases, and microbial activity decreases to very small rates compared to the growing season [*Björkman et al.*, 2010]. The low microbial activity at subzero soil temperatures can be studied in incubation experiments. Such laboratory studies have shown significantly stronger temperature responses of fluxes below 0°C than above, which could be due to the change of available liquid water [*Panikov et al.*, 2006], and/or the reduced transport capability of the frozen soil [*Elberling and Brandt*, 2003]. Cold season fluxes of CH_4 and CO_2 are therefore expected to be very small, but as this season prevails for a large part of the year in the Arctic, these small fluxes can still be an important contribution to the annual carbon balance [*Fahnestock et al.*, 1999; *Panikov and Dedysh*, 2000; *Aurela et al.*, 2002; *Lüers et al.*, 2014; *Smagin and Shnyrev*, 2015; *Zona et al.*, 2016]. Since cold season fluxes are difficult to measure in situ, there are still many open questions about the characteristics and controls of the emissions: Is the large spatial variability observed during the growing season also present in the cold season? Are the fluxes controlled by the same parameters, such as soil wetness and plant species composition, and are the gas sources caused by the same microbial production processes during the cold and the growing season?

One way to accurately measure the small cold season fluxes is to quantify the vertical gas concentration gradient in the snowpack, which can be related to the source strength in the soil using diffusion theory [*Sommerfeld et al.*, 1993; *McDowell et al.*, 2000; *Seok et al.*, 2009; *Maier and Schack-Kirchner*, 2014; *Smagin and Shnyrev*, 2015]. Under stable conditions, it can be estimated that it takes approximately 1 day to establish a stationary concentration profile in a porous snowpack [*Smagin and Shnyrev*, 2015], so that the expected temporal source variability can in principle be resolved. In this context, there is still uncertainty about the effect of the snowpack on the gas transport [*Bowling and Massman*, 2011]. Is the snowpack merely a passive cap, through which gases diffuse out into the atmosphere, or is there biological activity in the snowpack that affects emissions, as suggested by significant abundances of living microbes in Arctic snow [*Amato et al.*, 2007]? Moreover, what is the typical size of the snowpack gas reservoir in high Arctic wetlands, which could be released in sudden burst events during a storm or snowmelt [*Sullivan et al.*, 2012]?

We investigated these questions in two permafrost-underlain wetlands located in Northeast Greenland and Svalbard, respectively. Gas measurements were taken along transects parallel to sets of automatic flux chambers used in the snow-free period to study seasonal flux dynamics in relation to soil wetness, snowpack density, and isotopic source signature. We used a back-of-the-envelope temperature model to compare the observed fluxes with expectations and discuss estimates of the annual carbon budgets.

2. Materials and Methods

2.1. Study Sites

The site in Zackenberg Valley (74°30′N, 21°00′W) in the Northeast Greenland National Park lies in a region with a mean annual air temperature of −7.8°C (1996–2005), a ground thermal regime characterized by continuous permafrost, and a total annual precipitation of on average 286 mm [*Hansen et al.*, 2008]. Maximum snow depths vary interannually between 0.13 and 1.33 m [*Pedersen et al.*, 2016]. The measurement site is located on the edge of a fen and covers a wetness gradient stretching from the dry fringe of the fen into the wet center. The vegetation is dominated by *Eriophorum scheuchzeri*, *Carex* cf. *stans*, *Dupontia psilosantha*, and moss species.

The study site in Adventdalen Valley (78°11′N, 15°55′E) on Svalbard is located on the lower part of a large fan covered with eolian sediments. Active low-centered ice-wedge polygons are widespread in this continuous permafrost area creating fen conditions with shallow ponds in the study area [*Christiansen*, 2005; *Harris et al.*, 2009]. The region's mean annual air temperature is −3.75°C (2000–2011) [*Christiansen et al.*, 2013], and the average total annual precipitation is 190 mm, of which about half falls as snow [*Førland et al.*, 2012]. The snow is largely redistributed by wind, as is typical for such valleys on Svalbard [*Winther et al.*, 2003], leading to an average snow depth of only around 20 to 30 cm. The maritime setting causes changeable winter conditions in Adventdalen with large temperature variations ranging from around −30°C to warm spells slightly above 0°C. The warm spells can cause partial snow melt and be accompanied by rain events, both of which produce

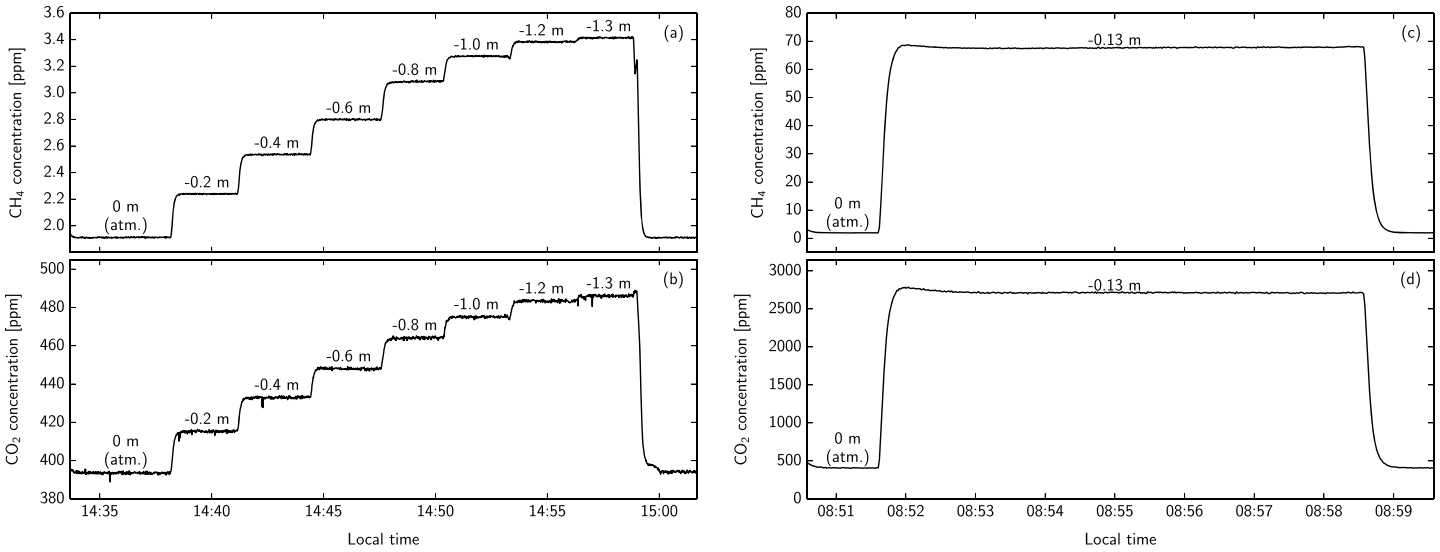

Figure 1. Gas concentration time series of CH_4 and CO_2 measured during the stepwise probing of the snowpack (depths indicated on each level). Zackenberg, 30 April 2012, transect position 6.45 m (a, b). Adventdalen, 11 April 2015, transect position 29 m, where only one layer could be probed (c, d).

solid ice layers in the snowpack upon refreezing. The vegetation at this site features *Salix polaris* in drier spots, *Eriophorum scheuchzeri*, and *Carex subspathacea* in wet locations, and moss species in usually inundated areas.

2.2. Snowpack Measurements

We conducted two campaigns at Zackenberg (2012 and 2014) and one in Adventdalen (2015) during the late cold season (April–May), featuring measurements of snowpack gas concentrations and manual closed chamber fluxes along transects parallel to a set of automatic flux chambers that are used during the snow-free period (see section 2.3). At Zackenberg (2012 and 2014) this transect was about 2 m offset the line of automatic flux chambers, about 20 m long and was sampled approximately every 2 m between mid-April and early June (see Figure S1 in the supporting information for a picture of a cold season campaign). Since this transect stretches from the dry fringe of the fen into its wet center, we associate every sampling point with a relative soil wetness given by the linear spatial interpolation between the end points of the transect, which define the minimum and maximum relative soil wetness. During summertime we monitor the water level both manually on a fixed scale and with divers installed in the ground at multiple positions on the transect, confirming this gradient in soil wetness. In the Adventdalen 2015 campaign, a 45 m long transect was sampled at 25 positions, but due to logistical limitations, this was done only once (on 10/11 April 2015). We complemented these gas measurements with ancillary data collected in the vicinity of the transects, such as wind speed, snow and ground temperature, and snow density (taken with sampling tubes in the walls of snow pits).

For the snowpack probing, a small probe equipped with a filter cap was inserted vertically into the snowpack to extract gas from individual snow layers at a flow rate of 0.4 L min^{-1}. High-density polyethylene tubes (4 mm inner diameter) connected the probe to a gas analyzer (Fast Greenhouse Gas Analyzer, Los Gatos Research, USA) which measured CH_4 and CO_2 concentrations (dry mole fractions) at a rate of 1.0 Hz. The measured gas concentrations (in ppm) were converted to mass densities using atmospheric air pressure and temperature measurements of the ambient air (for closed chamber method) and of snowpack profiles (for concentrations in the snowpack). During the 2014 campaign at Zackenberg, we measured the snowpack's stable isotope ratio of ^{12}C-CH_4 and ^{13}C-CH_4 (expressed in the $\delta^{13}C$ notation relative to VPDB) instead of CO_2, using a Methane Carbon Isotope Analyzer (Los Gatos Research, USA). The snowpack probing was performed stepwise from the top to the bottom of the snowpack, leaving the probe at the same position for several minutes. Since the snowpack in Adventdalen featured several ice layers we used a small drill to make holes for the probing. Figure 1 shows typical time series of gas concentrations generated by this procedure. For the analysis we used mean and standard deviation over 1 min of measurements on each respective level, i.e., 60 individual concentration measurements.

The gas concentration levels can be used to estimate the diffusive flux of the respective gas through the snowpack using Fick's law. Assuming steady state conditions, the vertical gas flux (q) is proportional to the gradient of the gas concentration (c) with depth (z), i.e.,

$$-q = D_{\text{eff}} \frac{\mathrm{d}c}{\mathrm{d}z}. \tag{1}$$

Here the effective gas diffusivity (D_{eff}) can be decomposed into the gases' diffusivity in air (D_0), the snowpack porosity (ϕ) and tortuosity (τ), i.e.,

$$D_{\text{eff}} = \phi\, \tau\, D_0 \left(\frac{P_0}{P}\right)\left(\frac{T}{T_0}\right)^{1.75}, \tag{2}$$

where D_0 (1.96×10^{-5} and 1.39×10^{-5} $m^2\ s^{-1}$, for CH_4 and CO_2, respectively) is given at a reference temperature ($T_0 = 273.15$ K) and pressure ($P_0 = 1013.3$ hPa) and scaled to ambient pressure (P) and snowpack temperature (T) following *Fuller et al.* [1966]. Porosity was derived from manual snow density measurements taken in snow pits in the vicinity. Here we estimated porosity directly from the ratio of measured snow density and ice density and therefore assume the liquid water content to be negligible. Considering the snowpack as an isotropic granular porous medium, tortuosity can be estimated from the measured porosity following *Du Plessis and Masliyah* [1991], i.e., $\tau = \frac{1-(1-\phi)^{\frac{2}{3}}}{\phi}$.

D_{eff} can vary through the snowpack, and specifically with depth z. If these variations are negligible, q can be estimated from a linear fit to the gradient of the entire gas concentration profile (as is done in the present study). Given the high precision of our gas analyzers, the main uncertainties in this flux estimation are likely to stem from nonstationary conditions (caused by, e.g., strong wind mixing atmospheric air into the top snow layer) and porosity changes in the snowpack (such as ice layers) [*Seok et al.*, 2009; *Smagin and Shnyrev*, 2015]. However, such physical processes affect both gas species equally, which means that the flux ratio becomes directly proportional to the vertical gradient ratio, i.e.,

$$\frac{q_{CH_4}}{q_{CO_2}} \propto \frac{\frac{\mathrm{d}c_{CH_4}}{\mathrm{d}z}}{\frac{\mathrm{d}c_{CO_2}}{\mathrm{d}z}}. \tag{3}$$

The δ^{13}C-CH_4 measurements with the given analyzer require the chemical removal of ambient CO_2 and H_2O, because these gases have similar absorption peaks that interfere with the ^{12}C-CH_4 and ^{13}C-CH_4 concentration measurements. We used the supplied removal kit of the manufacturer which kept CO_2 and H_2O concentrations below 30 and 20 ppm, respectively. For the data analysis, the snowpack CH_4 reservoir can be assumed to be a mixture of the atmospheric background and the CH_4 source in the soil, so that the Keeling approach can be applied to determine the isotopic signature of the CH_4 source [*Keeling*, 1958]. This source signature carries information about microbial production and oxidation, because different metabolic processes fractionate the carbon in characteristic ways [*Hornibrook et al.*, 2000; *Chanton et al.*, 2004].

We conducted manual closed chamber flux measurements of CH_4 and CO_2 on the same spots where the snowpack gas profiles were taken afterward, using transparent chambers with base dimensions of 25 cm by 25 cm, and a height of 15 cm (Zackenberg 2012 and 2014) and 21 cm (Adventdalen 2015). At Zackenberg, where the snowpack was soft enough, we fitted the chamber to a frame that went approximately 10 cm into the snowpack, while no frame was used on the dense snowpack in Adventdalen, where the chamber edge went into the snowpack just enough to ensure the acceptable sealing from ambient air. A fan was used for gas mixing and reflective foil was placed around the chamber on sunny days to prevent chamber headspace temperature from increasing. We used closure times of at least 20 min, from which fluxes were calculated using ordinary least squares linear regression. While the choice of regression model constitutes one of the largest sources of systematic uncertainty [*Kutzbach et al.*, 2007; *Levy et al.*, 2011], the local flux variability is typically equally well captured in linear and curvilinear models [*Pirk et al.*, 2016].

2.3. Automatic Closed Chamber Measurements

During snow-free periods, we conducted measurements of CH_4 and CO_2 (and δ^{13}C-CH_4 at Zackenberg 2014) using automatically operated flux chambers [*Goulden and Crill*, 1997] connected to the same gas analyzers as used in the snowpack measurements. The present study uses data from 2012 and 2014 at Zackenberg (10 chambers) and 2015 from Adventdalen (3 chambers). All chambers are transparent with base dimensions of 60 cm by 60 cm, a height of 30 cm, and a fan for gas mixing. The effective free volume in the chamber

headspace is manually monitored on a regular basis and accounted for in the flux calculation. The automatic protocol of the system subsequently activates the individual chambers and takes the flux measurements with 5 min closure time (see *Mastepanov et al.* [2013] for details). The flux calculation is again based on ordinary least squares linear regression, which is applied to the time window yielding the highest R^2 and verified by visual inspection. This procedure resulted in flux time series with 2 and 1 h resolution from each chamber for Zackenberg and Adventdalen, respectively.

2.4. Modeling of Cold Season Fluxes

If cold season fluxes are driven by instantaneous microbial gas production in the frozen soil, we expect the fluxes to depend on soil temperature and substrate availability. To be able to compare the measured cold season fluxes to these expectations, we calculated theoretical flux time series based on empirical temperature response functions found in incubation laboratory experiments, and in situ measured ground temperatures (5 cm depth). In this scheme, the microbial decomposition of organic material that drives the fluxes of CH_4 and CO_2 is assumed to follow an exponential temperature relationship, which is typically expressed as a Q_{10} value (factor of increase upon a 10°C temperature increase). Below 0°C, *Panikov and Dedysh* [2000] report Q_{10} values from 5 to 10 for CH_4. For CO_2, *Panikov et al.* [2006] report a Q_{10} of 4.5, using temperature as the only predictor. Accordingly, we here chose $Q_{10}(CH_4) = 7.5 \pm 2.5$ and $Q_{10}(CO_2) = 4.5 \pm 1.5$ and only applied the model during frozen ground conditions. We used the same soil temperature time series for all locations on the measured transects. The spatial discrimination of the fluxes stems from the location-specific substrate pool and scaling of the temperature response function.

Accordingly, we normalized these temperature response functions to the expected gas flux at 0°C, which is exponentially extrapolated from the automatic chamber measurements taken during the month before soil freezing starts (see Figure S6 in the supporting information for details of the parameter determination). We furthermore assume that the substrate driving microbial decomposition in the cold season only consists of the freshly assimilated carbon of the previous growing season. We quantify this substrate pool as the cumulated net ecosystem exchange measured by the automatic flux chambers during the growing season (see Figure S7 in the supporting information for the time series of a model run). This estimation scheme neglects much of the complexity of the different decomposition pathways, so the quantified substrate pool can only be regarded as a simplified proxy for the actual microbial substrates, and the modeled fluxes become a first-order approximation. A more technical description of this model is provided in Text S1 in the supporting information.

3. Results

3.1. Snowpack Gas Concentrations

During the stepwise probing of the snowpack, the gas concentrations stayed on stable levels over several minutes of measurements indicating that the characterized gas volumes in the snow comprised several liters of air. Figure 2a shows a typical example of the derived CH_4 concentration levels for the snowpack at Zackenberg, 25 May 2012. The relative soil wetness of each position on the transect is indicated by the colors used in the figure (the same color scheme is used throughout all figures from Zackenberg). Figure 2b gives the corresponding CO_2 concentrations. For CH_4, the vertical gradients clearly depend on soil wetness, whereas the CO_2 gradients show less spatial variability on the measured transect (relative standard deviation of concentrations at the soil surface of 6% for CO_2, compared to 25% for CH_4). There seems to be a CO_2 emission hot spot toward the dry end of the measured transect that is absent in CH_4 (suggesting a change in the microbial community structure). Figure 2c shows the ratio of the vertical gradients of CH_4 and CO_2 for the same day and positions. Here physical effects (such as density variations due to a stratified snowpack or wind mixing at the surface) are largely eliminated, and the profiles are directly proportional to the ratio of fluxes, i.e., q_{CH_4}/q_{CO_2} (cf. equation (3)). The positions with the highest CH_4 concentrations showed a shift of q_{CH_4}/q_{CO_2} close to the soil surface (snow depth −1.0 m), which could be due to shoots of vascular plants that stick out 20 cm from the soil surface and open a pathway to a source deeper in the soil where more CH_4 than CO_2 is produced. However, we found no general trend of a decreasing relative q_{CH_4} toward the snow surface in our measurements, which otherwise would indicate a microbial CH_4 sink in the snowpack. Some of the vertical variations seen in the profiles of Figure 2c can also result from horizontal gas transport, which in some places can be almost as large as the vertical gas transport, as exemplified by the annotated arrows in Figure 2a indicating the horizontal and vertical CH_4 gradients between neighboring sampling points.

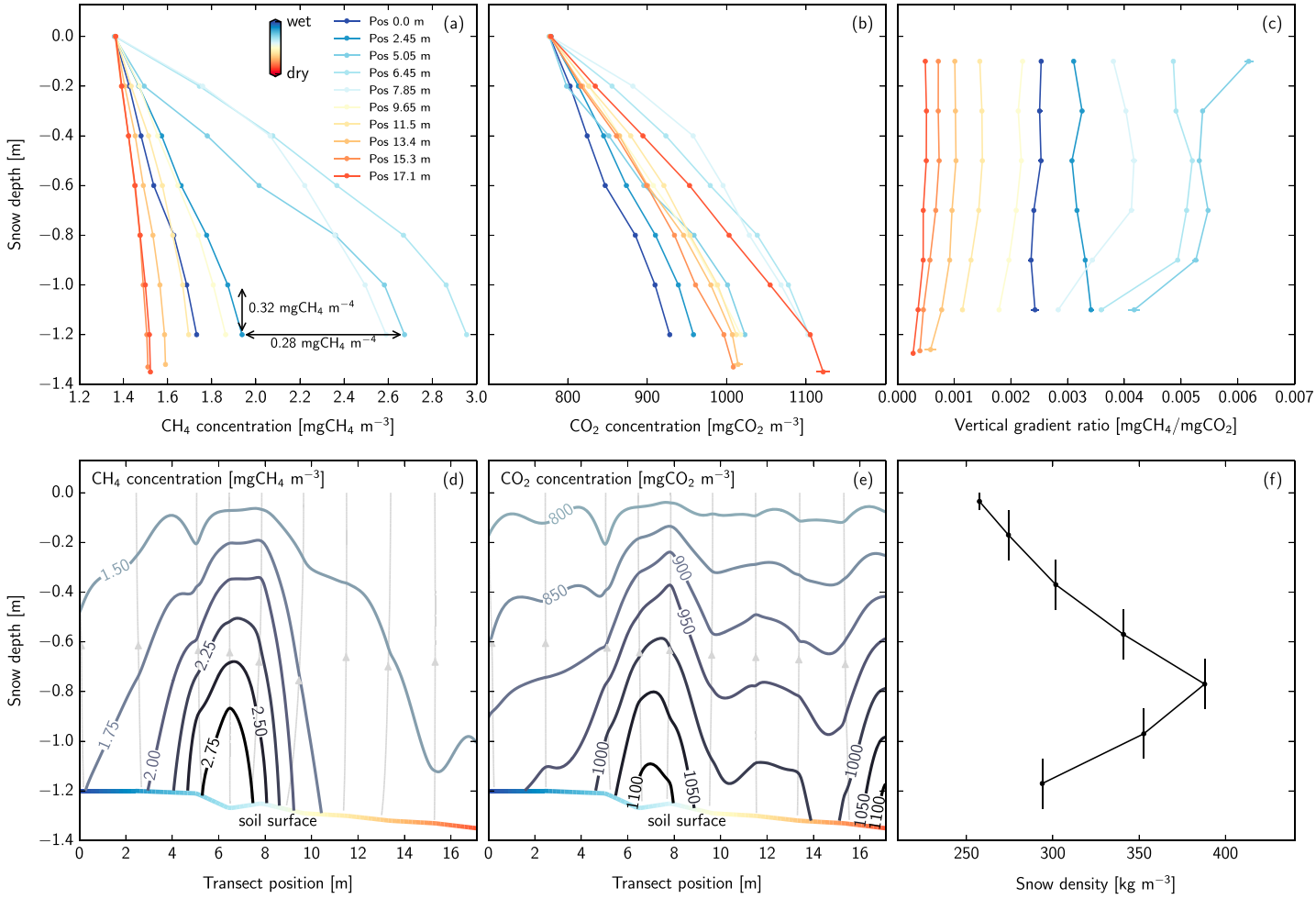

Figure 2. Example of the measured snowpack concentrations from Zackenberg, 25 May 2012. (a) CH_4 concentration profiles from the 10 positions on the transect, which are colored according to their relative soil wetness. Error bars indicate standard deviations around the mean at the respective level but are typically smaller than the marker size. The maximum of 3.0 mg CH_4 m^{-3} corresponds to 4.1 ppm CH_4. The annotated arrows indicate horizontal and vertical gradients between neighboring sampling points. (b) Corresponding CO_2 concentration profiles. The maximum of 1122 mg CO_2 m^{-3} corresponds to 556 ppm CO_2. (c) Resulting vertical gradient ratio (cf. equation (3)). (d) Snowpack cross section showing the interpolated CH_4 concentrations of Figure 2a as contours, and their negative gradients as streamlines. (e) Corresponding graph for CO_2. (f) Snow densities taken with a sampling tube in a snow pit 15 m offset the transect.

A more comprehensive illustration of the transport patterns can be given by concentration cross sections of the snowpack. Figures 2d and 2e show such cross sections of the snowpack based on the same gas concentrations as shown in Figures 2a and 2b, respectively. While the contour lines show the interpolated concentrations (using a cubic radial basis function), the streamlines indicate their negative gradients, i.e., the theoretical flow fields assuming diffusion in a homogenous snowpack. The resulting orthogonality between the gradient streamlines and the concentration isopleths is difficult to see in these figures because of the different scaling of x axis (∼17 m) and y axis (∼1.5 m). The spatial variability of the sources on the soil surface leads to horizontal gas transport, which is more pronounced for CH_4 than CO_2. The true source strengths on the soil surface will therefore be smeared out on the snow-atmosphere interface. Figure 2f shows the snow density, which was maximal at −0.8 m depth, from where it decreased approximately linearly toward both soil and snow surface. The snowpack thickness ranged between 1.2 and 1.4 m throughout the campaign at Zackenberg 2012, with an average density of 320 kg m^{-3}. Slightly shallower and denser snow conditions were observed at Zackenberg 2014 before snowmelt started (0.8 to 1.0 m depth, and 420 kg m^{-3} average density).

The snowpack in Adventdalen was much shallower and denser than at Zackenberg. On the probed transect shown in Figure 3a, the snowpack depths ranged from 13 to 33 cm, featuring several ice layers (see Figure S2 in the supporting information for a picture of a snow pit). Figure 3b shows the measured CH_4 and CO_2

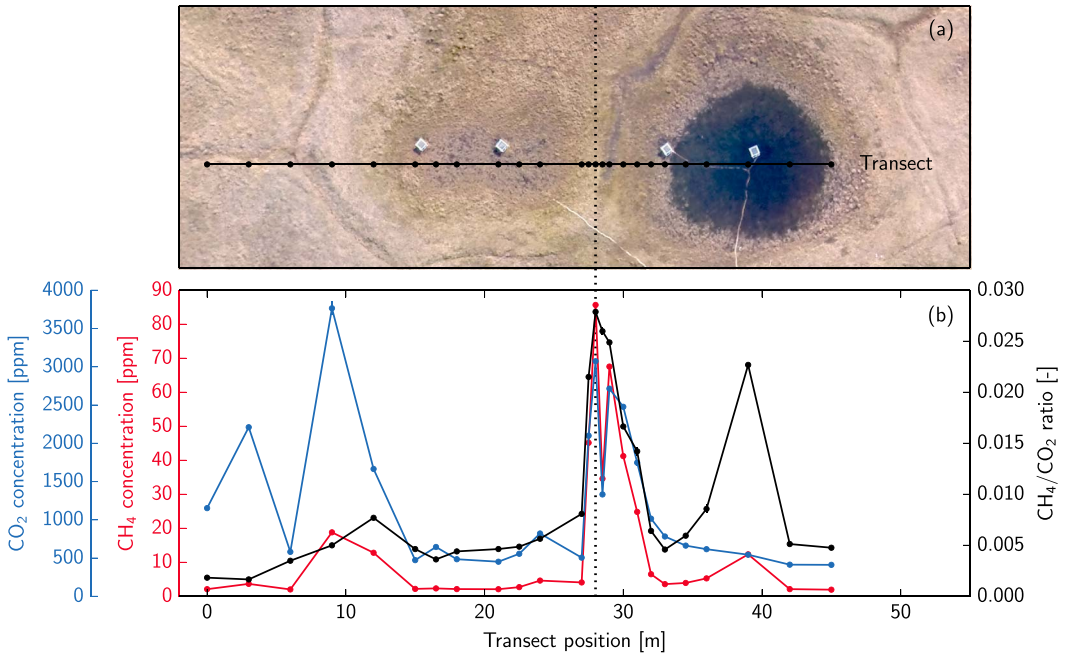

Figure 3. Probed transect parallel to four automatic flux chambers in the polygonal tundra of Adventdalen. (a) Sample positions on an aerial photography taken in June 2015. (b) Measured concentrations at full snowpack depth (at the soil surface) of CH_4 (red) and CO_2 (blue), as well as their ratio (black). Error bars indicate standard deviations around the mean at the respective level but are typically smaller than the marker size.

concentrations at full snow depth, which had large variations of up to 86 ppm CH_4 and 3800 ppm CO_2 at certain positions. While part of the variations can be attributed to physical changes in the local snowpack, the concentration ratio captures the source characteristics in the soil. Especially in the wetter part of the transect, this ratio resembles the polygonal pattern—with the highest relative CH_4 concentration on the rampart of the ice-wedge polygon.

3.2. Fluxes

Throughout all measurements, the concentrations of both gases strictly increased with depth, indicating small but measurable gas sources in the soil that gave rise to a diffusive flux toward the atmosphere. The vertical gas flux at the soil surface can differ from the flux between the snow surface and the atmosphere due to horizontal gas transport and nonstationary gas accumulation (cf. Figures 2 and 3). Figure 4 shows the comparison of the manual closed chamber fluxes at the snow surface and the diffusive flux estimates derived from the gas concentration gradient at the snowpack-atmosphere interface (−20 to 0 cm depth) for the campaign at Zackenberg 2012. The present scatter, as well as the slight tendency of lower manual closed chamber fluxes compared to diffusive gradient fluxes, demonstrates the degree of statistical and systematic uncertainty of our flux measurements (see also Figure S4 in the supporting information for comparisons using gradients of different layers in the snowpack). Flux computational uncertainties and gas flow disturbances by the two techniques can contribute to (and possibly dominate) both statistical and systematic errors, while uncertainties connected to the gas concentration measurements with the gas analyzers are probably less important for our flux estimates. As mentioned above, CH_4 fluxes exhibit larger relative variability than CO_2, so that the correlation between the methods is higher ($r = 0.83$ for CH_4 compared to $r = 0.57$ for CO_2).

At Zackenberg, the measured concentration gradients of the entire snowpack showed high degrees of linearity ($R^2 > 0.8$), indicating acceptable stationarity and the applicability of Fick's law (cf. equation (1)) for diffusive flux estimations of the cold season. There were indications that higher wind speed could increase the advection of snowpack gases and decrease R^2 of our linear fits (see Figure S5 in the supporting information), but the remarkably high degree of linearity of the gas concentration profiles motivates the diffusive flux estimation as the dominant gas transport mechanism. Figure 5 shows the compilation of the resulting flux time series for 2012, where the relative soil wetness of each position is indicated by the same color scheme as above. The gray band indicates the active layer freeze-in period, during which gas emission bursts can occur. At times

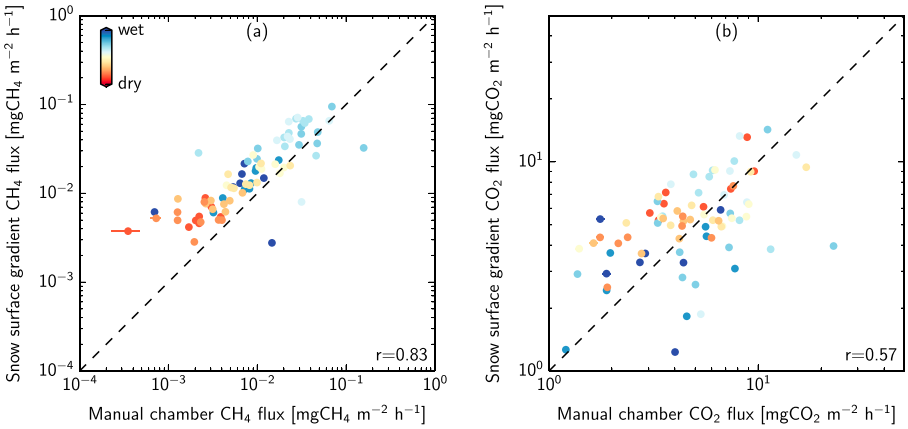

Figure 4. Comparison of manual closed chamber and snowpack gradient method (applied at the snow surface, −20 cm to 0 cm depth) for the campaign at Zackenberg 2012. (a) CH_4. (b) CO_2.

with concurrent measured and modeled results, relatively good agreement exists both in flux magnitude and the representation of the wetness gradient. There are larger differences between wet and dry positions in the Q_{10} temperature model compared to the measurements, which can in part be due to horizontal gas transport in the snowpack that smears out the source variability or other processes not captured by the model. For CH_4, the snowpack fluxes were found lowest at the driest locations, while the model predicted even lower fluxes for some medium-dry locations (yellow lines). Nevertheless, the results collectively show that the same spatial hierarchy of CH_4 source strengths is established on different orders of magnitude throughout the entire year. In fact, soil wetness affects the CH_4 emissions to such an extent, that the wetter positions show cold season emissions exceeding some of the growing season emissions from the drier positions.

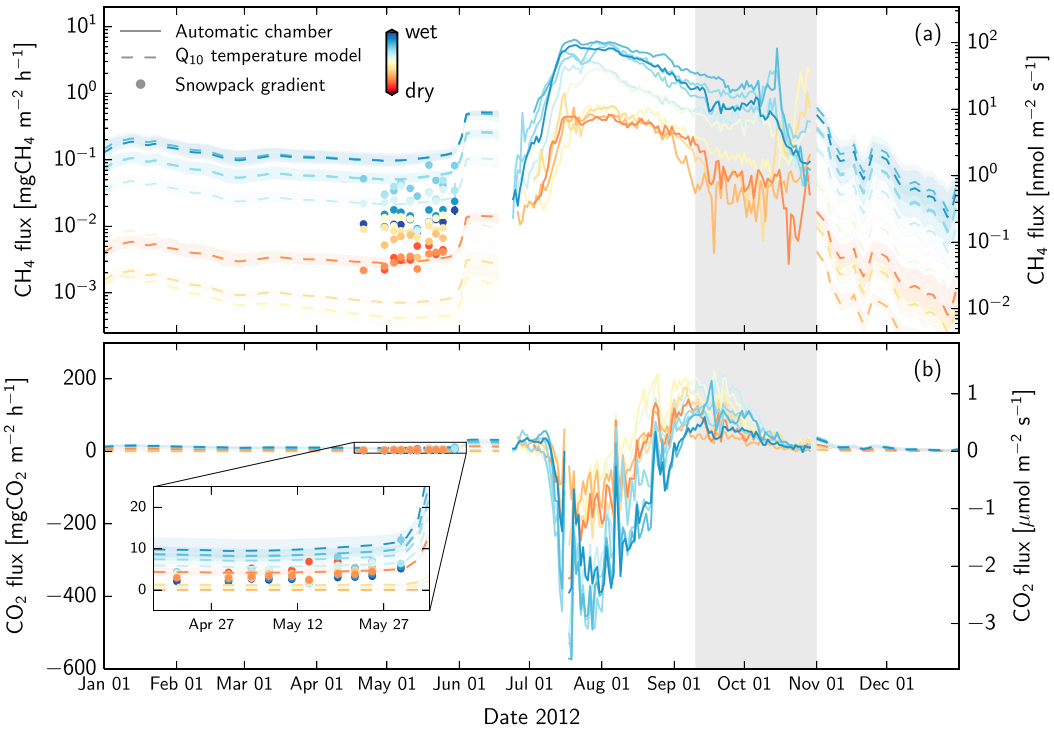

Figure 5. Flux time series from Zackenberg 2012 colored according to relative soil wetness. (a) CH_4 fluxes on logarithmic scale to bring out differences in the small cold season fluxes. (b) Corresponding CO_2 fluxes with an inset focusing on the cold season. Shaded bands around the model results indicate variations corresponding to the used range of Q_{10} values. The gray band indicates the soil freeze-in period, during which gas emission bursts can occur.

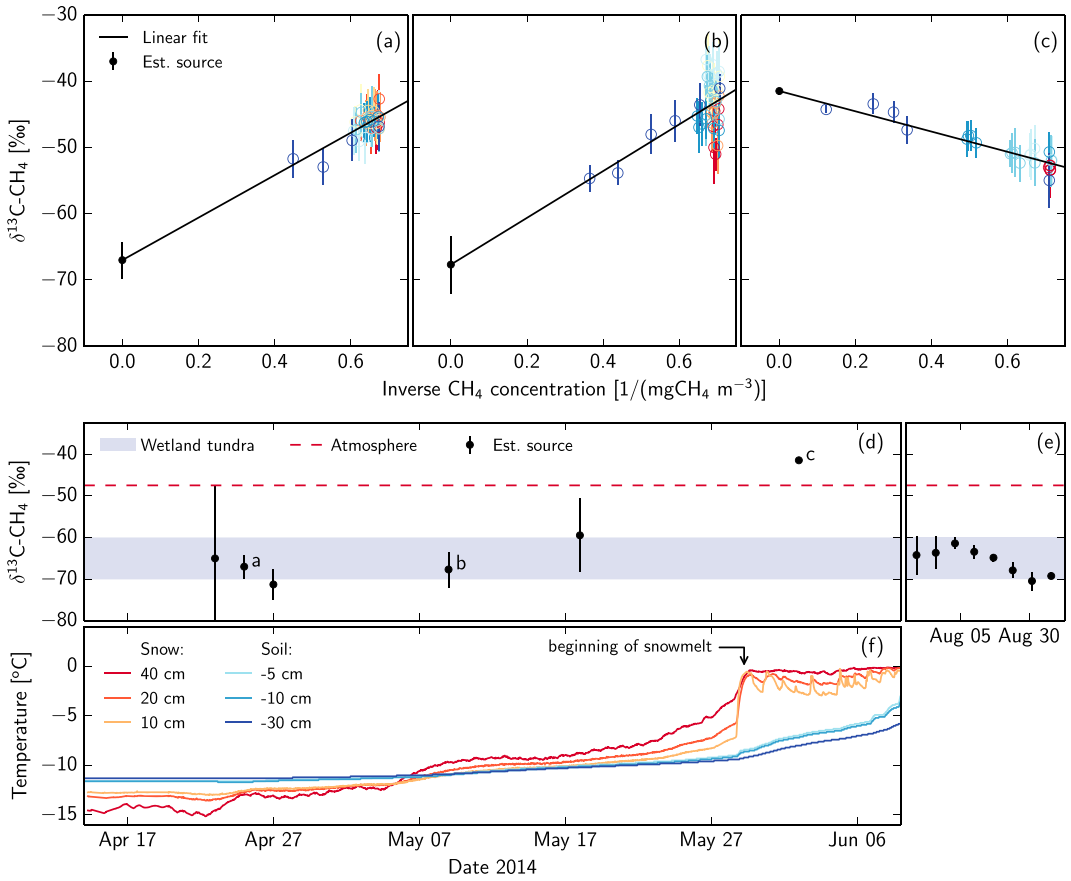

Figure 6. Stable isotope ratios of CH_4 at Zackenberg 2014. (a–c) Example Keeling plots from the snowpack probing from days annotated in Figure 6d. As above, colors indicate relative soil wetness of the position on the transect. (d) Time series of the source signatures derived from the snowpack probing. Wetland tundra and atmospheric reference values are taken from *Dlugokencky et al.* [2011]. (e) Corresponding signatures derived from automatic chamber data during the snow-free season. (f) Snow and soil temperatures indicating the period of snowmelt.

The effect of soil wetness on CO_2 fluxes is not as strong as for CH_4, but CO_2 cold season fluxes also tend to be higher in the wetter parts of the transect than in the drier parts. These findings were reproduced in the 2014 measurements from Zackenberg, even though cold season fluxes were slightly smaller on average (see Figure S8 in the supporting information).

In Adventdalen, snow surface fluxes from the manual closed chamber measurements were about 1 order of magnitude lower than expected from the Q_{10} temperature model (see Figure S8 in the supporting information). While this mismatch agrees well with the high gas concentrations found under the ice layers (see Figure 3), it may also indicate nonstationary conditions of the snowpack gas dynamics. Since the ice layers in the snowpack caused large inhomogeneities with highly nonlinear concentration gradients ($R^2 < 0.4$), we did not use the gradients for flux estimations and only report the manual closed chamber flux estimates, which were in the same range as the detection limit of this technique.

3.3. Isotopic Signature of CH_4 Source

In the snowpack measurements at Zackenberg 2014, we found that not only the CH_4 concentrations but also its isotopic signature changed with depth in the snowpack. The relationship between inverse CH_4 concentration and $\delta^{13}C\text{-}CH_4$ can be linearly extrapolated to estimate the CH_4 source signature (corresponding to an inverse CH_4 concentration of zero). Figures 6a–6c show examples of these Keeling plots, where particularly the wettest point on the probed transect (where CH_4 concentrations were highest) provides a suitable basis for the determination of the CH_4 source signature. While interferences of these measurements with remaining CO_2 or H_2O cannot be completely excluded, the linearity in the Keeling plots suggests the validity of the resulting source signatures within their statistical uncertainty. Figure 6d shows the resulting time series as well as

the typically expected signatures for tundra wetlands and ambient atmospheric air. To further compare these results with growing season data, Figure 6e shows the corresponding CH_4 source signatures derived from automatic chamber measurements during summer 2014. Throughout the late cold and growing season, most of the derived signatures fall in the band between −70 and −60‰, indicating that the same microbial processes invoke the CH_4 emissions. The significantly heavier signature (depleted in ^{12}C-CH_4) during snowmelt coincides with a total CH_4 flux at this position which is higher than expected from the model, suggesting the physical release of a gas reservoir that was subjected to different fractionation processes (see Figure S8 in the supporting information for total CH_4 flux time series).

4. Discussion

We investigated the snowpack gas dynamics of CH_4 and CO_2 in two high Arctic tundra wetlands to assess the controlling factors of cold season gas fluxes. We found increasing gas concentrations with depth at all locations, indicating small but measurable gas emissions from the soil. As these fluxes showed no decreasing trend throughout our campaigns over several months, it appears more like that the fluxes are driven by instantaneous gas production in the frozen soil instead of the mere release of the soil gas reservoir. The large spatial flux variability is also resembled in the cold season, where fluxes varied over orders of magnitude. Particularly for CH_4, soil wetness appears to be a year-round flux control, even though related site conditions influencing the substrate quality and quantity (such as the plant species composition) may be the underlying cause for the observed flux differences. Especially *Eriophorum scheuchzeri* increases CH_4 production and release through its root exudates supplying methanogenic substrates and efficient plant mediated transport in its aerenchyma, respectively [*Ström et al.*, 2005, 2015]. The highest gas emissions were, however, not always found at the highest soil wetness, so it seems as if the wettest locations on the transect may be suboptimal for these vascular plants, while slightly drier areas suit such plant species better.

Seok et al. [2009] found that strong winds significantly influence CO_2 concentrations and gradients in snowpacks, and there are reports of correspondingly increased gas exchange fluxes from high Arctic tundra ecosystems with considerable impacts on the annual carbon budget [*Lüers et al.*, 2014]. Our snowpack concentration measurements can quantify the size of such potential storm bursts in the late cold season. If, for example, a storm emptied the entire snowpack gas reservoir and replaced it with ambient atmospheric air during a short period of 30 min, the resulting fluxes at Zackenberg (approximately 1.2 m snow with a porosity of about 70%) would be around 1 mg CH_4 m^{-2} h^{-1} and 200 mg CO_2 m^{-2} h^{-1}. These hypothetical burst fluxes are roughly equal to actually observed fluxes in the late growing season (cf. Figure 5). Given the typical soil sources during the cold season, the snowpack gas reservoir would be largely filled up again after about 1 day after the burst. The shallow and dense snowpack in Adventdalen, which had on average higher gas concentrations than at Zackenberg, would allow for gas emission bursts of about twice the above mentioned numbers for Zackenberg. Still, these fluxes represent the highest conceivable upper limits, and real storm bursts from high Arctic wetlands may be much smaller because the snowpack gases would probably be released gradually over periods longer than 30 min. Similarly, gas contained within the snow will be released during snowmelt events, as observed at a site in northern Arizona [*Sullivan et al.*, 2012]. The thawing period in Zackenberg Valley has been found to exhibit increased CO_2 emission rates in years with a deep and long-lasting snowpack [*Lund et al.*, 2012]. Our calculations suggest that such increased emissions during snowmelt extending over several days cannot be due to the release of the snowpack gas storage alone but are more likely caused by processes occurring in the soil as well (release of gas storage or instantaneous production).

The systematic uncertainties of the different flux estimation techniques have not been included in the error bars shown in the figures above. When comparing snowpack gradient and closed chamber fluxes, studies from lower latitudes come to different conclusions: Some studies found CH_4 and CO_2 fluxes of both methods in good agreement [*Alm et al.*, 1999; *Kim et al.*, 2007], while others noted that estimates of wintertime fluxes can vary more as a result of the method used than actual variations in the soil gas production or release [*Björkman et al.*, 2010]. *Schindlbacher et al.* [2007] found higher CO_2 fluxes with the gradient method than the closed chamber method, which was attributed to lateral diffusion in the snowpack under the chamber. In contrast, *Rains et al.* [2016] found that the gradient method underestimated cold season CO_2 flux by at least 25% due to disregarded advection fluxes in the snowpack. *Bowling and Massman* [2011] used the stable isotopic composition of snowpack CO_2 to show that such nondiffusive, wind-driven gas transport increased diffusive CO_2 emissions by about 10% when integrated over an entire winter. In a review of the topic *Maier and Schack-Kirchner* [2014] therefore concluded that both snowpack gradient and closed chamber methods

are challenging to use in snow. In our study we also found it difficult to estimate the diffusive flux through the snowpack in Adventdalen with its shallow and dense snow cover. Such inhomogeneous snowpacks do not favor the gradient flux technique. At Zackenberg, however, we found both methods well suited to resolve the natural flux variability, as indicated by their good agreement in Figure 4. And while many flux measurement techniques can lose sensitivity at small flux magnitudes, our snowpack gradient estimates show no decrease of sensitivity even at the smallest source strengths. Extracting gas from the snowpack unavoidably induces a mass flow toward the intake probe which could disturb the natural gas gradients, but we consider this a minor problem because the size of the affected volume around the probe is estimated to be smaller than the sampling steps. We find that the dominating uncertainties of the gradient technique stem from variations in the snowpack porosity (in time and space) and wind-driven mixing of atmospheric air in the snowpack, as also noted by other studies [*Takagi et al.*, 2005; *Seok et al.*, 2009; *Maier and Schack-Kirchner*, 2014; *Smagin and Shnyrev*, 2015]. Since such physical processes affect both gas species equally, the flux ratio q_{CH4}/q_{CO_2} can be determined at much higher precision than the individual fluxes, so the flux ratio could in principle be used to constrain gas production or consumption by, e.g., methanotrophs in the snowpack. Such microbial activity with the capacity to degrade organic compounds has been found in various ice-rich environments [*Price*, 2007] and specifically in seasonal Arctic snow [*Amato et al.*, 2007], so there is a possibility for gas sources or sinks in the snowpack. However, the vertical concentration gradients measured in the snowpack at Zackenberg show no general trend in the ratio of CH_4 to CO_2 as these gases diffuse upward, which indicates that there are no significant biological gas sinks or sources inside the snowpack. Horizontal diffusion of gases in the snowpack complicate the determination of an upper limit for snowpack methanotrophy and could not be fully assessed with our two-dimensional probing scheme along transects. In the one horizontal dimension we resolved, diffusion in the snowpack was found to smear out the source variability at the soil surface. Still, the closed chamber measurements on the snow surface showed comparable spatial variations on the measured transect. Variations on larger scales are in principle difficult to assess in manual campaigns like ours and must be derived from models that parameterize the involved processes. Our results principally support such efforts, as is demonstrated by the realistic representation of flux magnitudes and spatial patterns by our simple Q_{10} temperature model.

The Q_{10} model is solely based on scaled temperature relationships (derived in incubation studies) combined with an estimate of the soil's fresh substrate pool. The assumed control of summertime productivity on wintertime fluxes is supported by *Zhao et al.* [2016], who measured significantly decreased (21% lower) wintertime CO_2 emissions in a northern Swedish peatland on plots that were artificially shaded in the preceding summer. Still, our model lacks a process-based description of the gas production and release, and as such neglects potentially relevant effects like changing Q_{10} values throughout wintertime, gas storage during which CH_4 could be oxidized to CO_2, or interannual variations of the substrate pool (which could also describe the decomposition of older carbon stocks). Despite these limitations and uncertainties, the Q_{10} model describes the measured snowpack fluxes relatively well, which motivates an assessment of the total annual flux budgets based on the Q_{10} temperature model and the measured automatic chamber fluxes. Figure 7 shows the cumulative flux time series for Zackenberg 2011–2012 and 2013–2014. Both years show the same characteristic picture, even though exact numbers differ slightly. The largest total annual CH_4 source in the wet part of the transect amounted to $7.1^{+0.1}_{-0.1}$ g C m^{-2} in 2011–2012 (given uncertainty represents Q_{10} value range), of which about 15% stemmed from the cold season (November–May) and an almost equal 14% from freeze-in period (September–October). In the dry part of the transect, total CH_4 emissions amounted to only about $0.40^{+0.0001}_{-0.0001}$ g C m^{-2}, with similar relative contributions from the cold season and freeze-in period as in the wetter areas. These numbers are very much in line with *Wille et al.* [2008], who found 35% CH_4 flux contribution from wintertime (October–May) in polygonal tundra in the Lena delta, much of which was attributed to the long freeze-in period. The same was concluded from measurements on the Alaskan Arctic tundra, where more than 50% of the annual CH_4 budget stemmed from the wintertime (September–May) [*Zona et al.*, 2016]. In contrast, a temperate peatland with an only 3 month long winter was found to only emit about 4% of its annual CH_4 emissions during wintertime [*Melloh and Crill*, 1996]. For CO_2, cold season emissions at Zackenberg were found to be close to 0 g C m^{-2} on the dry part of the transect, and up to 27^{+5}_{-3} g C m^{-2} on the wet part. This difference is also reflected in the total annual CO_2 budget, which is positive (source) in the dry part and negative (sink) in the wet part. So the cold season's small but consistent CO_2 emissions can be significant for the total carbon budget of these ecosystems, which is typically rather small [*Webb et al.*, 2016].

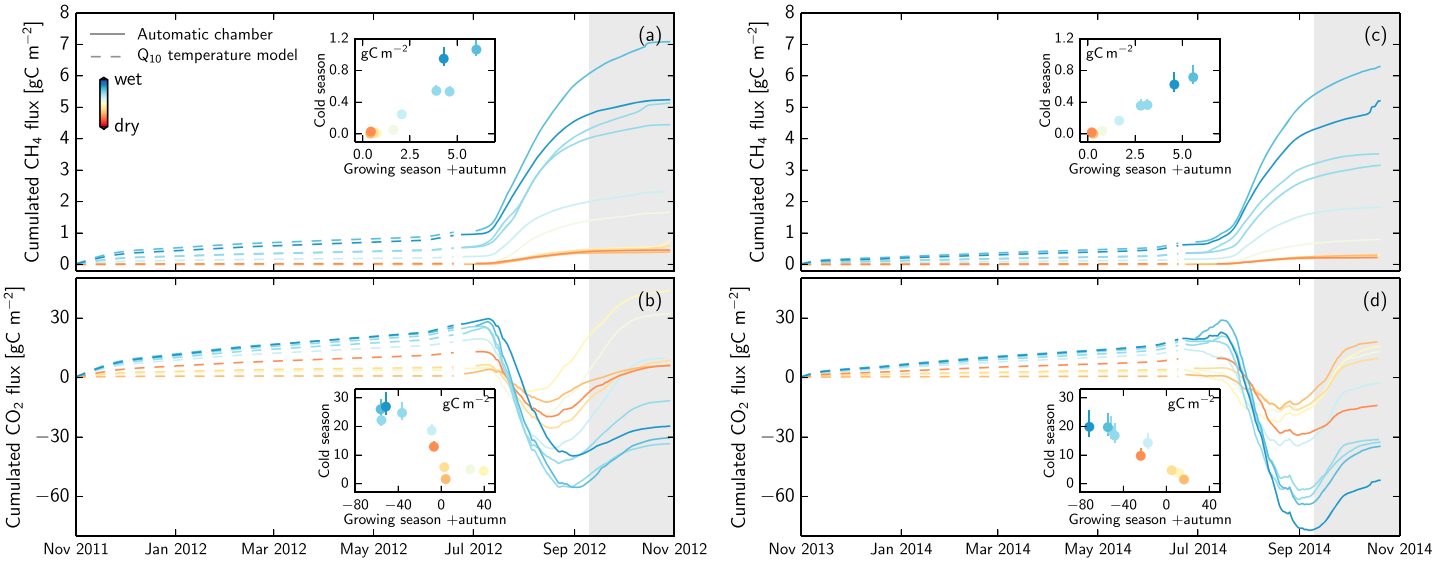

Figure 7. Cumulated fluxes for a 1 year period at Zackenberg (a, b) 2011–2012 and (c, d) 2013–2014, for both CH_4 (Figures 7a and 7c) and CO_2 (Figures 7b and 7d). The gray band indicates the soil freeze-in period, during which gas emission bursts can occur. The inset graphs show comparisons of the respective contributions from the cold season (November–May), and the growing season and autumn freezeup (June–October). Error bars indicate variations corresponding to the range of Q_{10} values.

At the ice-wedge polygon site in Adventdalen, the situation was complicated by ice layers in the snowpack that effectively blocked the diffusive gas transport. *Melloh and Crill* [1995] report similar observations from a temperate fen, where concentrations of up to 600 ppm CH_4 were measured underneath an ice layer in the snowpack. Ice layers of only a few millimeters thickness can lower the gas permeability of a snowpack by about 1 order of magnitude compared to fresh seasonal snow [*Albert and Perron*, 2000], while on the other hand even very thick ice layers have some degree of permeability [*Domine et al.*, 2008]. Given the expected soil gas source in Adventdalen, the highest measured snowpack concentrations could therefore have taken between 1 week and 1 month to accumulate. And while the timing of ice layer formation may be estimated from meteorological time series, it remains uncertain if and how the snowpack reservoirs may be released into the atmosphere, and what their effect on the total annual budget may be. More advanced modeling efforts (where transport mechanisms are included) would be needed to come to an understanding of the cold season's effect on the annual carbon budget. Growing season CH_4 emissions from other polygonal tundra sites showed substantial small-scale variability which was related to the hydrological conditions within the microrelief of the polygon [*Kutzbach et al.*, 2004; *Vaughn et al.*, 2016]. Our results indicate that there are similar spatial variations of the gas sources during the cold season. Interestingly, the strongest relative CH_4 source was found in the rampart of the polygons, at 1.5 m distance from the polygon trough above the ice wedge. Ice wedges are known to support relatively high microbial activity [*Wilhelm et al.*, 2012], and they open in wintertime due to thermal contraction cracking down through the active layer and into the top of the permafrost [*Christiansen*, 2005]. The adjacent ramparts are the most elevated parts at the site and can feature centimeter-wide surface cracks, which are formed as the soil is pushed up during ice-wedge expansion in winter and in summer when the entire polygon expands [*Christiansen*, 2005]. And while no centimeter-wide crack was seen at the respective rampart upon visual inspection in summer 2015, a smaller fissure could already have closed again during polygon expansion. Nearby ice-wedge polygons with more developed ramparts show many examples of such cracks, which were large enough to be visible during summertime (see example in Figure S3 in the supporting information). These soil cracks appear to be hot spots for the emission of CH_4 and CO_2. If such geomorphological gas flux controls are widespread in permafrost-underlain tundra, their large-scale effect (also in summertime) could be considerable since ice-wedge polygons are estimated to worldwide cover about 250,000 km^2 in an area with large, potentially labile, carbon stocks [*Minke et al.*, 2007; *Hugelius et al.*, 2014].

As mentioned above, our data show no clear signs of a hypothetical CH_4 sink due to methanotrophs consuming CH_4 on its way through the snowpack. Rather, the CH_4 reservoir stored in the frozen soil might be subject to consumption by methanotrophs. Our stable isotope measurements indicate a CH_4 source signature which is significantly heavier (depleted in ^{12}C-CH_4) during snowmelt when the uppermost soil starts thawing.

One conceivable mechanism is the release of a gas reservoir in the thawing surface soil that was trapped for a long time in exposure to methanotrophs, which preferably utilize the lighter ^{12}C-CH_4 isotope and thereby increase $\delta^{13}C$-CH_4 [*Chanton et al.*, 2004; *Preuss et al.*, 2013]. Such cold season soil methanotrophy could in some cases explain the absence of large spring bursts of CH_4, which would be expected if the strong apparent temperature dependence of subzero gas emissions was largely due to physical trapping of the produced gases [*Elberling and Brandt*, 2003]. Apart from the pulse during snowmelt, the isotopic signature of the CH_4 source in the cold season was largely the same as during the growing season, suggesting that CH_4 emissions result from the same microbial processes all year round, which has similarly been observed in temperate wetland ecosystems [*Hornibrook et al.*, 2000].

We only covered a part of the interannual variability, as the investigated years at Zackenberg (2012 and 2014) were both similarly snow rich [*Pedersen et al.*, 2016], and wintertime weather in Adventdalen is typically highly variable. Our methods have proven to be well suited for snowpack flux studies, so more such measurement campaigns could be conducted to further integrate our findings in a general description. Such future studies should also aim to measure snowpack gas dynamics in the autumnal early snow period and try to cover a larger range of soil temperatures to verify its effect on cold season fluxes.

5. Conclusions

We found small but measurable greenhouse gas sources in two high Arctic tundra ecosystems during the late cold season. The relatively low temporal resolution of our dedicated measurement campaigns only motivated a back-of-the-envelope modeling of wintertime fluxes, which are therefore still associated with large uncertainties. While the cold season (November–May) only contributed moderately to the annual CH_4 budget, its small but consistent CO_2 emissions can be significant for the total carbon budget of these ecosystems. Horizontal gas transport, which can locally be as large as vertical transport, smeared out the local variations of the soil gas sources and limited our ability to constrain potential methanotrophy in the snowpack. Our study shows that wintertime greenhouse gas emissions from permafrost-underlain tundra are affected by soil wetness—controlling substrate accumulation and microbial activity—methanotrophy in the soil gas reservoir, ice layers in the snow, and geomorphological surface cracking. Since conditions such as soil wetness may carry over from one season to the other, we conclude that the growing season and the cold season should not be considered independently but rather continuously to assess the greenhouse gas exchange of high Arctic tundra environments.

Acknowledgments
The data underlying our conclusions is provided in the figures of this article and its supporting information. Raw measurement data and processing scripts are available from the authors upon request (norbert.pirk@nateko.lu.se). Data from the Greenland Ecosystem Monitoring Program were provided by the Department of Bioscience, Aarhus University, Denmark, in collaboration with Department of Geosciences and Natural Resource Management, Copenhagen University, Denmark. We thank Jordan Mertes for providing the aerial photography of the ice-wedge site in Adventdalen. The research leading to these results has received funding from the European Community's Seventh Framework Program (FP7) under grants 238366, 262693, and 282700; the Nordic Centers of Excellence DEFROST and eSTICC (eScience Tool for Investigating Climate Change in northern high latitudes) funded by Nordforsk (grant 57001); the GeoBasis programs supported by the Danish Energy Agency; and the Arctic Research Centre, Aarhus University.

References

Albert, M. R., and F. E. Perron (2000), Ice layer and surface crust permeability in a seasonal snow pack, *Hydrol. Processes*, *14*(18), 3207–3214.
Alm, J., S. Saarnio, H. Nykänen, J. Silvola, and P. Martikainen (1999), Winter CO_2, CH_4 and N_2O fluxes on some natural and drained boreal peatlands, *Biogeochemistry*, *44*(2), 163–186.
Amato, P., R. Hennebelle, O. Magand, M. Sancelme, A.-M. Delort, C. Barbante, C. Boutron, and C. Ferrari (2007), Bacterial characterization of the snow cover at Spitzberg, Svalbard, *FEMS Microbiol. Ecol.*, *59*(2), 255–264.
Aurela, M., T. Laurila, and J.-P. Tuovinen (2002), Annual CO_2 balance of a subarctic fen in northern Europe: Importance of the wintertime efflux, *Journal of Geophysical Research: Atmospheres*, *107*(D21), 4607, doi:10.1029/2002JD002055.
Björkman, M. P., E. Morgner, E. J. Cooper, B. Elberling, L. Klemedtsson, and R. G. Björk (2010), Winter carbon dioxide effluxes from Arctic ecosystems: An overview and comparison of methodologies, *Global Biogeochem. Cycles*, *24*, GB3010, doi:10.1029/2009GB003667.
Bowling, D. R., and W. Massman (2011), Persistent wind-induced enhancement of diffusive CO_2 transport in a mountain forest snowpack, *J. Geophys. Res. Biogeosc.*, *116*, G04006, doi:10.1029/2011JG001722.
Chanton, J., L. Chaser, P. Glasser, and D. Siegel (2004), Carbon and hydrogen isotopic effects in microbial methane from terrestrial environments, in *Stable Isotopes and Biosphere-Atmosphere Interactions, Physiological Ecology Series*, pp. 85–105, Elsevier Acad. Press, London.
Christensen, T. R., A. Ekberg, L. Ström, M. Mastepanov, N. Panikov, M. Öquist, B. H. Svensson, H. Nykänen, P. J. Martikainen, and H. Oskarsson (2003), Factors controlling large scale variations in methane emissions from wetlands, *Geophys. Res. Lett.*, *30*(7), 1414, doi:10.1029/2002GL016848.
Christiansen, H. H. (2005), Thermal regime of ice-wedge cracking in Adventdalen, Svalbard, *Permafrost Periglacial Process.*, *16*(1), 87–98.
Christiansen, H. H., O. Humlum, and M. Eckerstorfer (2013), Central Svalbard 2000–2011 meteorological dynamics and periglacial landscape response, *Arct. Antarct. Alp. Res.*, *45*(1), 6–18.
Dlugokencky, E. J., E. G. Nisbet, R. Fisher, and D. Lowry (2011), Global atmospheric methane: Budget, changes and dangers, *Philos. Trans. R. Soc. A*, *369*(1943), 2058–2072.
Domine, F., M. Albert, T. Huthwelker, H.-W. Jacobi, A. Kokhanovsky, M. Lehning, G. Picard, and W. Simpson (2008), Snow physics as relevant to snow photochemistry, *Atmos. Chem. Phys.*, *8*(2), 171–208.
Du Plessis, J. P., and J. H. Masliyah (1991), Flow through isotropic granular porous media, *Transport Porous Media*, *6*(3), 207–221.
Elberling, B., and K. K. Brandt (2003), Uncoupling of microbial CO_2 production and release in frozen soil and its implications for field studies of Arctic C cycling, *Soil Biol. Biochem.*, *35*(2), 263–272.
Fahnestock, J. T., M. H. Jones, and J. M. Welker (1999), Wintertime CO_2 efflux from Arctic soils: implications for annual carbon budgets, *Global Biogeochem. Cycles*, *13*(3), 775–779.

Førland, E. J., R. Benestad, I. Hanssen-Bauer, J. E. Haugen, and T. E. Skaugen (2012), Temperature and precipitation development at Svalbard 1900–2100, *Adv. Meteorol.*, *2011*, 893790.

Fuller, E. N., P. D. Schettler, and J. C. Giddings (1966), New method for prediction of binary gas-phase diffusion coefficients, *Ind. Eng. Chem.*, *58*(5), 18–27.

Goulden, M., and P. Crill (1997), Automated measurements of CO_2 exchange at the moss surface of a black spruce forest, *Tree Physiol.*, *17*(8-9), 537–542.

Hansen, B. U., C. Sigsgaard, L. Rasmussen, J. Cappelen, J. Hinkler, S. H. Mernild, D. Petersen, M. P. Tamstorf, M. Rasch, and B. Hasholt (2008), Present-day climate at Zackenberg, *Adv. Ecol. Res.*, *40*, 111–150.

Harris, C., et al. (2009), Permafrost and climate in Europe: Monitoring and modelling thermal, geomorphological and geotechnical responses, *Earth Sci. Rev.*, *92*(3), 117–171.

Hornibrook, E., F. Longstaffe, and W. Fyfe (2000), Factors influencing stable isotope ratios in CH_4 and CO_2 within subenvironments of freshwater wetlands: Implications for δ-signatures of emissions, *Isotopes Environ. Health Studies*, *36*(2), 151–176.

Hugelius, G., et al. (2014), Estimated stocks of circumpolar permafrost carbon with quantified uncertainty ranges and identified data gaps, *Biogeosciences*, *11*(23), 6573–6593.

Keeling, C. D. (1958), The concentration and isotopic abundances of atmospheric carbon dioxide in rural areas, *Geochim. Cosmochim. Acta*, *13*(4), 322–334.

Kim, Y., M. Ueyama, F. Nakagawa, U. Tsunogai, Y. Harazono, and N. Tanaka (2007), Assessment of winter fluxes of CO_2 and CH_4 in boreal forest soils of central Alaska estimated by the profile method and the chamber method: A diagnosis of methane emission and implications for the regional carbon budget, *Tellus B*, *59*(2), 223–233.

Kutzbach, L., D. Wagner, and E.-M. Pfeiffer (2004), Effect of microrelief and vegetation on methane emission from wet polygonal tundra, Lena Delta, Northern Siberia, *Biogeochemistry*, *69*(3), 341–362.

Kutzbach, L., J. Schneider, T. Sachs, M. Giebels, H. Nykänen, N. Shurpali, P. Martikainen, J. Alm, and M. Wilmking (2007), CO_2 flux determination by closed-chamber methods can be seriously biased by inappropriate application of linear regression, *Biogeosciences*, *4*(6), 1005–1025.

Lai, D. (2009), Methane dynamics in northern peatlands: A review, *Pedosphere*, *19*(4), 409–421.

Levy, P., A. Gray, S. Leeson, J. Gaiawyn, M. Kelly, M. Cooper, K. Dinsmore, S. Jones, and L. Sheppard (2011), Quantification of uncertainty in trace gas fluxes measured by the static chamber method, *Eur. J. Soil Sci.*, *62*(6), 811–821.

Lüers, J., S. Westermann, K. Piel, and J. Boike (2014), Annual CO_2 budget and seasonal CO_2 exchange signals at a High Arctic permafrost site on Spitsbergen, Svalbard archipelago, *Biogeosciences*, *11*(22), 6307–6322.

Lund, M., J. M. Falk, T. Friborg, H. N. Mbufong, C. Sigsgaard, H. Soegaard, and M. P. Tamstorf (2012), Trends in CO_2 exchange in a high Arctic tundra heath, 2000–2010, *J. Geophys. Res.*, *117*, G02001, doi:10.1029/2011JG001901.

Maier, M., and H. Schack-Kirchner (2014), Using the gradient method to determine soil gas flux: A review, *Agricul. Forest Meteorol.*, *192*, 78–95.

Mastepanov, M., C. Sigsgaard, E. J. Dlugokencky, S. Houweling, L. Ström, M. P. Tamstorf, and T. R. Christensen (2008), Large tundra methane burst during onset of freezing, *Nature*, *456*(7222), 628–630.

Mastepanov, M., C. Sigsgaard, T. Tagesson, L. Ström, M. P. Tamstorf, M. Lund, and T. Christensen (2013), Revisiting factors controlling methane emissions from high-Arctic tundra, *Biogeosciences*, *10*, 5139–5158, doi:10.5194/bg-10-5139-2013.

McDowell, N. G., J. D. Marshall, T. D. Hooker, and R. Musselman (2000), Estimating CO_2 flux from snowpacks at three sites in the Rocky Mountains, *Tree Physiol.*, *20*(11), 745–753.

McGuire, A., et al. (2012), An assessment of the carbon balance of Arctic tundra: Comparisons among observations, process models, and atmospheric inversions, *Biogeosciences*, *9*, 3185–3204, doi:10.5194/bg-9-3185-2012.

Melloh, R. A., and P. M. Crill (1995), Winter methane dynamics beneath ice and in snow in a temperate poor fen, *Hydrol. Processes*, *9*(8), 947–956.

Melloh, R. A., and P. M. Crill (1996), Winter methane dynamics in a temperate peatland, *Global Biogeochem. Cycles*, *10*(2), 247–254.

Minke, M., N. Donner, N. S. Karpov, P. de Klerk, and H. Joosten (2007), Distribution, diversity, development and dynamics of polygon mires: Examples from Northeast Yakutia (Siberia), *Peatlands Int.*, *1*, 36–40.

Olefeldt, D., M. R. Turetsky, P. M. Crill, and A. D. McGuire (2013), Environmental and physical controls on northern terrestrial methane emissions across permafrost zones, *Global Change Biol.*, *19*(2), 589–603.

Olsson, P. Q., M. Sturm, C. H. Racine, V. Romanovsky, and G. E. Liston (2003), Five stages of the Alaskan Arctic cold season with ecosystem implications, *Arct. Antarct. Alp. Res.*, *35*(1), 74–81.

Panikov, N., P. Flanagan, W. Oechel, M. Mastepanov, and T. Christensen (2006), Microbial activity in soils frozen to below −39C, *Soil Biol. Biochem.*, *38*(4), 785–794.

Panikov, N. S., and S. Dedysh (2000), Cold season CH_4 and CO_2 emission from boreal peat bogs (West Siberia): Winter fluxes and thaw activation dynamics, *Global Biogeochem. Cycles*, *14*(4), 1071–1080.

Pedersen, S. H., et al. (2016), Spatiotemporal characteristics of seasonal snow cover in Northeast Greenland from in situ observations, *Arct. Antarct. Alp. Res.*, doi:10.1657/AAAR0016-028.

Pirk, N., T. Santos, C. Gustafson, A. J. Johansson, F. Tufvesson, F.-J. W. Parmentier, M. Mastepanov, and T. R. Christensen (2015), Methane emission bursts from permafrost environments during autumn freeze-in: New insights from ground penetrating radar, *Geophys. Res. Lett.*, *42*, 6732Ű6738, doi:10.1002/2015GL065034.

Pirk, N., M. Mastepanov, F.-J. W. Parmentier, M. Lund, P. Crill, and T. R. Christensen (2016), Calculations of automatic chamber flux measurements of methane and carbon dioxide using short time series of concentrations, *Biogeosciences*, *13*, 903–912, doi:10.5194/bg-13-903-2016.

Preuss, I., C. Knoblauch, J. Gebert, and E.-M. Pfeiffer (2013), Improved quantification of microbial CH_4 oxidation efficiency in Arctic wetland soils using carbon isotope fractionation, *Biogeosciences*, *10*, 2539–2552, doi:10.5194/bg-10-2539-2013.

Price, P. B. (2007), Microbial life in glacial ice and implications for a cold origin of life, *FEMS Microbiol. Ecol.*, *59*(2), 217–231.

Rains, F. A., P. C. Stoy, C. M. Welch, C. Montagne, and B. L. McGlynn (2016), A comparison of methods reveals that enhanced diffusion helps explain cold-season soil CO_2 efflux in a lodgepole pine ecosystem, *Cold Regions Sci. Technol.*, *121*, 16–24.

Schimel, J. P. (1995), Plant transport and methane production as controls on methane flux from Arctic wet meadow tundra, *Biogeochemistry*, *28*(3), 183–200.

Schindlbacher, A., S. Zechmeister-Boltenstern, G. Glatzel, and R. Jandl (2007), Winter soil respiration from an Austrian mountain forest, *Agric. Forest Meteorol.*, *146*(3), 205–215.

Seok, B., D. Helmig, M. W. Williams, D. Liptzin, K. Chowanski, and J. Hueber (2009), An automated system for continuous measurements of trace gas fluxes through snow: An evaluation of the gas diffusion method at a subalpine forest site, Niwot Ridge, Colorado, *Biogeochemistry*, *95*(1), 95–113.

Smagin, A., and N. Shnyrev (2015), Methane fluxes during the cold season: Distribution and mass transfer in the snow cover of bogs, *Eurasian Soil Sci.*, *48*(8), 823–830.

Sommerfeld, R., A. Mosier, and R. Musselman (1993), CO_2, CH_4 and N_2O flux through a Wyoming snowpack and implications for global budgets, *Nature*, *361*, 140–142.

Ström, L., M. Mastepanov, and T. R. Christensen (2005), Species-specific effects of vascular plants on carbon turnover and methane emissions from wetlands, *Biogeochemistry*, *75*(1), 65–82.

Ström, L., J. M. Falk, K. Skov, M. Jackowicz-Korczynski, M. Mastepanov, T. R. Christensen, M. Lund, and N. M. Schmidt (2015), Controls of spatial and temporal variability in CH_4 flux in a high Arctic fen over three years, *Biogeochemistry*, *125*(1), 21–35.

Sturtevant, C. S., and W. C. Oechel (2013), Spatial variation in landscape-level CO_2 and CH_4 fluxes from Arctic coastal tundra: Influence from vegetation, wetness, and the thaw lake cycle, *Global Change Biol.*, *19*(9), 2853–2866.

Sullivan, B. W., S. Dore, M. C. Montes-Helu, T. E. Kolb, and S. C. Hart (2012), Pulse emissions of carbon dioxide during snowmelt at a high-elevation site in Northern Arizona, USA, *Arct. Antarct. Alp. Res.*, *44*(2), 247–254.

Takagi, K., M. Nomura, D. Ashiya, H. Takahashi, K. Sasa, Y. Fujinuma, H. Shibata, Y. Akibayashi, and T. Koike (2005), Dynamic carbon dioxide exchange through snowpack by wind-driven mass transfer in a conifer-broadleaf mixed forest in northernmost Japan, *Global Biogeochem. Cycles*, *19*, GB2012, doi:10.1029/2004GB002272.

Vaughn, L. J. S., M. E. Conrad, M. Bill, and M. S. Torn (2016), Isotopic insights into methane production, oxidation, and emissions in Arctic polygon tundra, *Global Change Biol.*, *22*, 3487–3502, doi:10.1111/gcb.13281.

Webb, E. E., E. A. Schuur, S. M. Natali, K. L. Oken, R. Bracho, J. P. Krapek, D. Risk, and N. R. Nickerson (2016), Increased wintertime CO_2 loss as a result of sustained tundra warming, *J. Geophys. Res. Biogeosci.*, *121*, 249–265, doi:10.1002/2014JG002795.

Whalen, S. (2005), Biogeochemistry of methane exchange between natural wetlands and the atmosphere, *Environ. Eng. Sci.*, *22*(1), 73–94.

Wilhelm, R. C., K. J. Radtke, N. C. Mykytczuk, C. W. Greer, and L. G. Whyte (2012), Life at the wedge: The activity and diversity of Arctic ice wedge microbial communities, *Astrobiology*, *12*(4), 347–360.

Wille, C., L. Kutzbach, T. Sachs, D. Wagner, and E. Pfeiffer (2008), Methane emission from Siberian Arctic polygonal tundra: Eddy covariance measurements and modeling, *Global Change Biol.*, *14*(6), 1395–1408.

Winther, J.-G., O. Bruland, K. Sand, S. Gerland, D. Marechal, B. Ivanov, P. Gøowacki, and M. König (2003), Snow research in Svalbard – An overview, *Polar Res.*, *22*(2), 125–144.

Zhao, J., M. Peichl, M. Öquist, and M. B. Nilsson (2016), Gross primary production controls the subsequent winter CO_2 exchange in a boreal peatland, *Global Change Biol.*

Zona, D., et al. (2016), Cold season emissions dominate the Arctic tundra methane budget, *Proc. Natl. Acad. Sci.*, *113*(1), 40–45.